Femtosecond laser pulse control of electron transfer processes

Tomáš Mančal
Institut für Physik, Humboldt-Universität zu Berlin, Hausvogteiplatz 5-7, D-10117 Berlin, Germany

Ulrich Kleinekathöfer
Institut für Physik, Technische Universität, D-09107 Chemnitz, Germany

Volkhard May
Institut für Physik, Humboldt-Universität zu Berlin, Hausvogteiplatz 5-7, D-10117 Berlin, Germany

(Received 25 February 2002; accepted 8 April 2002)

Laser-pulse guided ultrafast electron transfer (ET) is studied theoretically for different types of donor–acceptor systems. The pulse initiates an optical transition from the electronic ground state into an excited state and controls the ET. The computations concentrate on systems where (a) the excited state (donor) is coupled to an acceptor level and where (b) the ET proceeds as an internal conversion from the excited state to the ground state. For both examples the manifold of vibrational coordinates is mapped on a single reaction coordinate coupled to a dissipative reservoir of further coordinates. Utilizing the methods of dissipative quantum dynamics combined with the optimal control (OC) scheme, it is demonstrated that control fields really exist which drive the ET in the required manner. Various properties of the OC algorithm are discussed when applied to dissipative dynamics and a scheme is proposed to avoid pinning in a local extremum. © *2002 American Institute of Physics.* [DOI: 10.1063/1.1481856]

I. INTRODUCTION

The proposal of laser-pulse control of molecular dynamics dates back to the middle of the eighties and has its origin in more or less completely theoretical considerations. A comprehensive overview on all attempts discussed so far has been given recently in Ref. 1. Originally suggested as several different approaches like the pioneering Tannor, Kosloff, and Rice scheme[2] or the coherent control scheme of Brumer and Shapiro,[3] the theory of laser-pulse control has been put into a universal frame by Rabitz in suggesting the so-called optimal control (OC) theory.[4,5] The OC theory is based on a certain functional which extremum has to be found. Once this extremum has been calculated, the shape is known of the laser pulse which drives the system in the desired manner. The functional consists of the expectation value of the observable one wants to maximize, e.g., the population of a particular state, and a constraint which restricts the pulse energy to a finite value. Originally, the OC theory has been formulated for gas-phase systems, which dynamics are governed by the time-dependent Schrödinger equation.[4,5] A formulation for mixed states could be already achieved in Ref. 6. The extension to reduced state dynamics of an open quantum system has been given in Ref. 7, and recently in Ref. 8 by extending the efficient iteration scheme of Refs. 9 and 10.

Meanwhile, experiments on femtosecond laser-pulse control of molecular dynamics became a subject of active physicochemical research.[11–14] Most of the work has been concentrated on the central idea of controlling chemical reactions resulting in a destruction or formation of a selected chemical bond. And indeed, a number of promising examples already exists even in the condensed phase.[15] While direct strategies to achieve the control goal have been applied in an earlier state of this research,[1] it was an experimental breakthrough to use highly flexible optical pulse-shaping systems combined with self-learning algorithms as suggested in Ref. 16.

Although this type of approach found a widespread experimental application, the use of self-learning algorithm in theory would remain on a preliminary level. This is because of the enormous amount of computational time necessary for carrying out the multitude of dynamic propagations. Consequently, it is much more appropriate to apply the OC theory whenever a control experiment has to be simulated. This conclusion leads to the problem of different experimental and theoretical constraints influencing the search for the optimal laser pulse. Therefore, the task for the theory is twofold. It has to solve the control task and it has to prove if the obtained pulse really fits the constraints present in the particular experiment. On the one-hand side one can try to include into the simulations the experimental conditions like the laser field spatial profile,[17] or the limited spectral width of the experimental pulses. Or alternatively, one can solve the control task without any experimental constraint and, afterwards, ask to what extent the pulse can be realized in the experiment.[18]

In the present paper we will follow the latter strategy in searching for a solution of the control task by means of the OC theory. In doing so we expect to get a general impression on the way the control of our particular molecular system becomes possible. In which manner one has to discuss the realization in an experiment is explained in Ref. 18 and will not be repeated here. The concrete type of dynamics, in which control should be studied in the following is related to ultrafast electron transfer (ET) reactions in donor–acceptor (DA) systems. There is a certain amount of theoretical literature on the external field control of ET.[19–25] These studies,

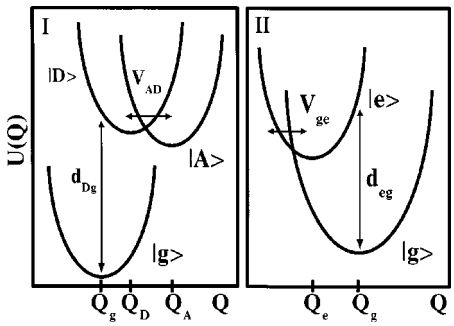

FIG. 1. PES of the studied model systems. ET model I: a donor–acceptor system typical for photoinduced ET. ET-model II: a system showing ET in the inverted regime after photoinduced charge separation into an excited state. The electronic transfer coupling (nonadiabatic coupling) and the optical transition are indicated by horizontal and vertical arrows, respectively.

however, do not deal with photoinduced ET reactions but with a type of external field control characterized by the action of a high-frequency electric field which modulates the energetic distance between the donor and the acceptor level. In contrast, the following studies are aimed to demonstrate the control of ET reactions by fields in the optical region. The energy level schemes we have in mind are shown in Fig. 1. A ground-state potential-energy surface (PES) is coupled to an excited state PES by an optical excitation. This excited state PES may couple to a further (acceptor) PES (model I) or via an internal conversion process to the ground state PES (model II). In any case the coupling lets the electron move away from the initially populated state. To control this motion by means of the exciting pulse, the coupling to the final state PES should be strong enough to introduce a sufficient large level mixing. This indicates that the reaction should be beyond the nonadiabatic type of ET and should be ultrafast, i.e., in the subpicosecond time domain.

A preliminary discussion of laser-pulse control of ET has been already given in Ref. 26. Here we generalize the discussion to include vibrational energy dissipation. A common approach to do this is to account for the coupling of the active (reaction) coordinates to a reservoir of passive vibrational coordinates (see e.g., Refs. 27–29 and the various contributions in Ref. 30). In this manner one includes frictional effects acting on the reaction coordinate and the ET has to be described in the framework of dissipative quantum dynamics (density matrix theory[29,31–34]).

As a potential candidate for realizing laser-pulse control of ET, we mention here the perylene molecule attached to the surface of the semiconductor TiO_2. For this system heterogeneous ET (into the semiconductor) which proceeds on a 100 fs time scale has been observed,[35,36] and can be well simulated in models which will be used here, too.[37–39] Although we have such a system in mind, the present studies concentrate on the models given in Fig. 1. The discussion of more involved models, including the continuum of PES, which refer to the band states of the semiconductor, is under work.

II. ULTRAFAST ELECTRON TRANSFER DYNAMICS

A. The electron transfer model

A common model for the description of ultrafast photoinduced ET is given by a set of electronic levels which are defined versus a small set of vibrational (reaction) coordinates.[29] The schemes of PES which will be of interest in the following are shown in Fig. 1. Often it suffices to consider a single vibrational coordinate or two coordinates. But in any case to account for energy dissipation and dephasing, a coupling to passive vibrational coordinates forming a thermal reservoir becomes necessary. The respective Hamiltonian H_S (describing the active system S of electron-vibrational degrees of freedom) includes the molecular part H_{mol} and the coupling to the external field $H_F(t)$. The first contribution will be written as

$$H_{\mathrm{mol}}=\sum_{a,b}\ (\delta_{a,b}H_a+(1-\delta_{a,b})V_{ab})|\varphi_a\rangle\langle\varphi_b|. \tag{1}$$

For the PES scheme I of Fig. 1 the electronic quantum number a comprises the ground-state contribution $a=g$ as well as the donor and acceptor $a=D,A$. The coupling matrix elements V_{ab} only concern the donor and the acceptor. In contrast, a is reduced to the ground-state contribution $a=g$ and the single excited state contribution $a=e$ for scheme II of Fig. 1, and the coupling V_{eg} is responsible for internal conversion. All vibrational Hamiltonian H_a are written with dimensionless vibrational coordinates $Q=\{Q_j\}$

$$H_a=T_{\mathrm{vib}}+U_a^{(0)}+\sum_j\ \frac{\hbar\omega_j}{4}(Q_j-Q_j^{(a)})^2. \tag{2}$$

The minima and the mutual displacements of the respective PEs are denoted by $U_a^{(0)}$ and $Q_j^{(a)}$, respectively. Any single coordinate Q_j can be expressed by harmonic oscillator operators C_j and C_j^+ according to $Q_j=C_j+C_j^+$. Respective vibrational *eigenfunctions* of the Hamiltonian H_a read $|\chi_{aM}\rangle$ where M denotes the set of vibrational quantum numbers. Consequently, the complete electron-vibrational states are given by $|\chi_{aM}\rangle|\varphi_a\rangle$. For model I we also introduce the adiabatic states $|\psi_\alpha\rangle$ which diagonalize the electron-vibrational states of the donor–acceptor system

$$|\psi_\alpha\rangle=\sum_{aM}\ A_\alpha(aM)|\chi_{aM}\rangle|\varphi_a\rangle. \tag{3}$$

The external field part of the system Hamiltonian H_S is given by

$$H_F(t)=-\mathbf{E}(t)\hat{\mu}. \tag{4}$$

The dipole operator reads

$$\hat{\mu}=\mathbf{d}_{ag}|\varphi_a\rangle\langle\varphi_g|+\mathrm{h.c.}, \tag{5}$$

where the quantum number a of the transition dipole moment refers to D (model I) or to e (model II). In any case $\mathbf{d}_{ag}$ is taken to be independent on the Q_j (Condon approximation). The field is assumed to be linearly polarized but remains free otherwise.

The model is completed by a coupling of the set Q of active coordinates to remaining passive vibrational coordinates.[29,30] These coordinates are denoted by $Z=\{Z_\xi\}$ and act as a dissipative reservoir. They may belong to the ET system completely or to a surrounding solvent. The respective coupling Hamiltonian if expanded with respect to the electronic states reads $H_{\mathrm{S-R}}=\Sigma_{a,b}W_{ab}(Q,Z)|\varphi_a\rangle\langle\varphi_b|$. For

the following it suffices to consider the diagonal contributions only. Furthermore, we assume that $W_a(Q,Z)$ factorizes into a system and a reservoir part. Therefore, $H_{\mathrm{S-R}}$ reads similar to the multiple factorized *ansatz* of dissipative quantum dynamics (see, e.g., Ref. 29)

$$H_{\mathrm{S-R}}=\sum_a \mathcal{K}_a\Phi_a . \tag{6}$$

The part

$$\mathcal{K}_a=K_a(Q)|\varphi_a\rangle\langle\varphi_a|, \tag{7}$$

is exclusively defined in the state space of active system states, and

$$\Phi_a(Z)=\hbar\sum_\xi k_\xi(a)Z_\xi , \tag{8}$$

is defined in the reservoir state space. For the present purposes it suffices to take an expression linearized with respect to the reservoir coordinates.

B. Reduced density matrix description of electron transfer

Since laser-pulse control of ET reactions will be described in the framework of dissipative quantum dynamics[29,31–34] one has to define the reduced density operator

$$\hat{\rho}(t)=\mathrm{tr}_{\mathrm{R}}\{\hat{W}(t)\}. \tag{9}$$

This quantity is obtained from the complete nonequilibrium statistical operator $\hat{W}(t)$ via a trace operation restricted to the reservoir states. The time evolution of the reduced density operator is governed by a respective time evolution superoperator which acts according to

$$\hat{\rho}(t)=\mathcal{U}(t,t_0;\mathbf{E})\hat{\rho}(t_0), \tag{10}$$

where its **E**-dependence has been separately indicated to show that the electric field strength has been incorporated in the density operator equation.

Changing to the electron vibrational state representation, the density matrix follows according to

$$\rho_{aM,bN}(t)=\langle\chi_{aM}|\langle\varphi_a|\hat{\rho}(t)|\varphi_b\rangle|\chi_{bN}\rangle. \tag{11}$$

As explained in more detail in Appendix A the density matrix obeys the following equation-of-motion:

$$\begin{aligned}\frac{\partial}{\partial t}\rho_{aM,bN}(t)=&-\omega_{aM,bN}\rho_{aM,bN}(t)-\frac{i}{\hbar}\sum_{cK}\left(V_{ac}\langle\chi_{aM}|\chi_{cK}\rangle\rho_{cK,bN}(t)-V_{cb}\langle\chi_{cK}|\chi_{bN}\rangle\rho_{aMcK}(t)\right)\\&-\langle\chi_{aM}|\langle\varphi_a|\mathcal{D}\hat{\rho}(t)|\varphi_b\rangle|\chi_{bN}\rangle+\frac{i}{\hbar}\mathbf{E}(t)\sum_{cK}\left(\mathbf{d}_{ac}\langle\chi_{aM}|\chi_{cK}\rangle\rho_{cK,bN}(t)-\mathbf{d}_{cb}\langle\chi_{ck}|\chi_{bN}\rangle\rho_{aMcK}(t)\right).\end{aligned} \tag{12}$$

Here, the action of the vibrational Hamiltonian H_a has been translated to the presence of electron-vibrational energies $E_{aM}=\hbar\omega_{aM}$ (transition frequencies are denoted as $\omega_{aM,bN}$). Those terms which describe the transfer between different electronic levels (proportional to V_{ab} and $\mathbf{d}_{ab}$) cover Franck–Condon overlap integrals. A detailed expression for the dissipative part (electron-vibrational matrix elements of $\mathcal{D}\hat{\rho}$, where $\mathcal{D}$ denotes the dissipative superoperator) is given in Appendix A. When calculating these matrix elements, an additional difficulty arises. It is caused by the fact that the states $|\varphi_a\rangle|\chi_{aM}\rangle$ do not represent *eigenstates* of the related molecular Hamiltonian (model I); as well they do not depend on the applied field (model I and II). Therefore a direct calculation of the dissipative part becomes impossible since the substructure of the dissipative superoperator $\mathcal{D}$ contains the time-evolution operators $U_{\mathrm{S}}(t,t_0;\mathbf{E})$ formed by the *complete* system Hamiltonian H_{S}. First, let us account for the electric field-strength dependence of U_{S}. Fortunately, it could be shown in Ref. 40 that the resulting laser pulse modulation of vibrational lifetimes and dephasing rates only becomes predominant at a really high field strength. For those used in the following, we can neglect the effect. Once the field dependence of U_S has been removed, it remains the problem to formulate (for model I) the action of U_{S} in the diabatic representation. This is achieved in changing to the adiabatic states, Eq. (3), which diagonalize U_S. In this manner we do not involve the so-called diabatic damping approximation (where the dependence of the dissipation rates on the donor–acceptor coupling is neglected) since under certain conditions it may lead to completely wrong results.[41,42]

III. OPTIMAL CONTROL SCHEME FOR DISSIPATIVE MOLECULAR DYNAMICS

For the present purposes it suffices to choose the traditional formulation of a control task, i.e., to find the laser pulse which completely drives the system from an initial into a final state at a certain time t_f.[1] The only deviation from this standard scheme is the consideration of an open system where energy dissipation and dephasing may counteract the control field.

As it is well known OC theory is based on the introduction of a particular functional of the laser field. Its extremum

defines the so-called *optimal pulse* which solves the control task. In the present case of the control of dissipative dynamics it is given as[6]

$$J(t_f;\mathbf{E}) = O(t_f;\mathbf{E}) - \frac{1}{2}\int_{t_0}^{t_f} dt\lambda(t)\mathbf{E}^2(t). \tag{13}$$

The expectation value of the observable specified by the target operator $\hat{O}$ at time t_f reads (note the restriction of the trace formula to the active system state space):

$$O(t_f) = \mathrm{tr}_S\{\hat{O}\hat{\rho}(t_f)\}. \tag{14}$$

The second term on the right-hand side of Eq. (13) guarantees an upper limitation of the field intensity. (To let the field smoothly switch on and off the penalty factor $\lambda(t)$ has been taken as time-dependent.[43])

The extremum of the control functional Eq. (13) is obtained in setting the functional derivative with respect to the field strength equal to zero. Such a calculation has been demonstrated elsewhere[44] and results in the following functional equation in which the solution determines the optimal pulse:

$$\mathbf{E}(t) = \frac{\mathbf{K}(t_f,t;\mathbf{E})}{\lambda(t)}. \tag{15}$$

The so-called (vectorial) control kernel reads

$$\mathbf{K}(t_f,t;\mathbf{E}) = \frac{i}{\hbar}\mathrm{tr}_S\{\hat{O}\mathcal{U}(t_f,t;\mathbf{E})(\hat{\mu},\mathcal{U}(t,t_0;\mathbf{E})\hat{\rho}(t_0))_-\}. \tag{16}$$

It is obtained by propagating first the reduced density operator (under the presence of the external field) from the initial time t_0 up to an intermediate time $t \leqslant t_f$. Then, it becomes necessary to calculate a commutator defined via the dipole operator. Afterwards, the result has to be propagated from t to the final time t_f where the operator $\hat{O}$ acts.

To solve Eq. (15) a certain iteration procedure has to be applied. We will use the scheme suggested in Ref. 8 where an auxiliary density operator $\hat{\sigma}$ is introduced which has to be propagated back in time. Accordingly the control kernel is rewritten as

$$K(t_f,t;\mathbf{E}) = \frac{i}{\hbar}\,\mathrm{tr}_S\{\hat{\sigma}(t;\mathbf{E})(\hat{\mu},\hat{\rho}(t;\mathbf{E}))_-\}, \tag{17}$$

where the operator at the left part of the trace is given as

$$\hat{\sigma}(t;\mathbf{E}) = \tilde{\mathcal{U}}(t_f,t;\mathbf{E})\hat{O}. \tag{18}$$

It comprises a reverse propagation from the final time t_f back to the intermediate time t starting with $\hat{O}$ at $t=t_f$. Note that the time propagation superoperator $\tilde{\mathcal{U}}$ basically deviates from that introduced in Eq. (10) (see Appendix B and the discussion in Ref. 26). The separate propagation at $\hat{\sigma}$ and $\hat{\rho}$ leads to a fast converging iteration procedure based on nonlinear density matrix equations.[8] They follow if the direct appearance of the control field $\mathbf{E}$ via the field term is removed in the equations for $\hat{\rho}$ and $\hat{\sigma}$. Such a replacement becomes possible in using Eq. (15) and the expression (17) for the control kernel (for more details compare Ref. 26).

TABLE I. Parameters of the single-mode version of the ET models A-1 and A-2 introduced in Sec. II A. The transfer integrals among the three PES responsible for the ET have been taken as $V_{DB}=V_{BA}=0.03$ eV, and $V_{DA}=0$. The transition dipol moment d_{Dg} has been set equal to 12 D.

m	A-1) $U_m^{(0)}-U_g^{(0)}$	A-2) $U_m^{(0)}-U_g^{(0)}$	$\hbar\omega_{\mathrm{vib}}$	$Q^{(m)}$
g	0	0	0.1 eV	0
D	2 eV	2 eV	0.1 eV	3.2
A	1.85 eV	1.891 eV	0.1 eV	7.0

IV. DISCUSSION OF DIFFERENT CONTROL SCENARIOS

The numerical computations presented below try to attain the following two goals. First, the applicability of the OC algorithm for the case of dissipative dynamics should be discussed in detail. Second, the idea of laser pulse control of ET reactions should be illustrated for different types of transfer reactions proceeding in different types of systems.

The two ET models chosen for our studies have been already introduced in Sec. II A. The respective system parameters are given in Tables I and II. The ET model I which represents the simplest version of a donor–acceptor system showing photoinduced ultrafast ET[45] has been specified by two different sets of parameters: model I-1 with vibrational levels of the donor and the acceptor in a complete off-resonant position, and model I-2 with these levels in nearly resonant position. The ET model II refers to the $S_1 \rightarrow S_0$ internal conversion process observed in the photoinduced dynamics of betaine-30 (the parameters are taken from Ref. 46). Note that for all sets of parameters, and even in the case of room temperature conditions, the equilibrium population of the vibrational levels giving the initial state is almost exclusively restricted to the vibrational ground state. To have some reference cases at hand, we start the discussion in neglecting dissipations. Afterwards, details of the influence of dissipation on ET laser pulse control are discussed.

A. Absence of dissipation (ET Model I)

While neglecting the influence of a thermal environment, we can examine some general features of laser pulse control of ET. In particular we will concentrate on the controllability of the ET in dependence of the control pulse length. It is obvious that ET spontaneously proceeds between the donor and the acceptor of the type-I models if an (initial) electron-vibrational state has been prepared in the donor PES (probably after laser excitation). And it depends on the degree of dissipation if the electron remains at the acceptor after the ET took place or if it moves different times back and forth between the donor and the acceptor. In both cases the ET can

TABLE II. Parameters of the single-mode version of the ET model B introduced in Sec. II A. The transfer integrals among the three PES responsible for the ET have been taken as $V_{ge}=V_{eg}=0.31$ eV. The transition dipol moment d_{eg} has been set equal to 5.3 D.

m	$U_m^{(0)}-U_g^{(0)}$	$\hbar\omega_{\mathrm{vib}}$	$Q^{(m)}$
g	0	0.223 eV	0
D	1.305 eV	0.223 eV	−2.483

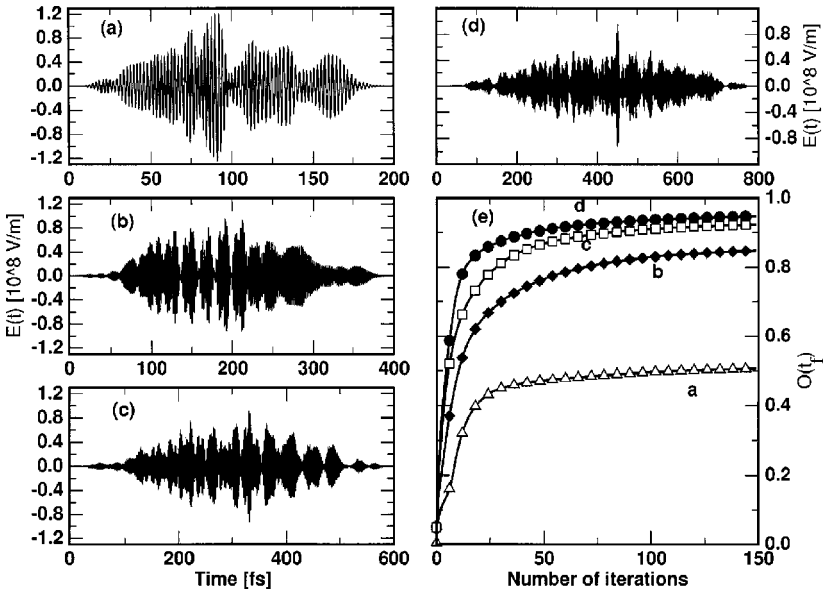

FIG. 2. Laser pulse control of ET for model I in the absence of dissipation (system parameters according to Table I part 2, target state: $|\varphi_A\rangle|\chi_{A1}\rangle$). The optimal pulse is shown for control tasks which differ with respect to their target time t_f. Panel a: $t_f=200$ fs, panel b: $t_f=400$ fs, panel c: $t_f=600$ fs, panel d: $t_f=800$ fs. The convergency behavior of the OC algorithm is shown in panel e.

be controlled by a particular shaping of the initial electron-vibrational wave packet. For weak dissipation a continuous formation of the electron-vibrational wave packet through the Franck–Condon window of the optical transition would control the ET. And in any case the target time t_f at which the electron should arrive at the target state must be comparable or longer than the time t_{ET} the electron needs to reach the acceptor without an external field influence. If $t_f > t_{ET}$ and if dissipation is weak enough or completely absent, the laser pulse may act within different cycles of the electron motion between the donor and the acceptor.

Figure 2 demonstrates that for $t_f > t_{ET}$ the OC yield can be increased if the number of the forth and back motion of the electron, i.e., if t_f is increased. Note, that the first excited vibrational state $|\varphi_A\rangle|\chi_{A1}\rangle$ at the acceptor PES has been taken as the target state. Besides the structure of the optimal pulse, Fig. 2 also shows the yield of the laser pulse control in dependence on the number of iteration steps within the OC algorithm. Here and in the following yield (control efficiency) is given by $O(t_f)$, Eq. (14), i.e., the degree to which the control task has been solved. The OC algorithm leads to a fast convergency into regions where more than 90% of the final value of $O(t_f)$ have been realized. This behavior may indicate that the chosen iterative procedure drives the solution of the optimization problem into a local minimum. If the ''surrounding'' of the local minimum is reached the convergency becomes weak. Furthermore, we emphasize the strong dependence of the control yield on details of the control task, here in particular on the chosen target time. A similar dependence on the target state could also be observed within other control tasks (see e.g., Ref. 18). This indicates that, besides the specificity of the molecular systems, also details of the control task can strongly affect the completeness by which the task may be solved by OC theory. We consider this as an additional hint for the property of the taken iteration scheme to fast reach a local minimum (Sec. IV D presents a further discussion on this problem).

B. Inclusion of vibrational relaxation (ET Model I)

In the present section we will study the way the presence of a thermal environment may influence the laser pulse control of those ET reactions discussed in the preceding section. Therefore, ET model I and the target state $|\varphi_A\rangle|\chi_{A1}\rangle$ are considered. But due to the action of the thermal environment all electron-vibrational states are characterized by a finite lifetime. In particular, the target state may decay into the acceptor vibrational ground state. To get an impression on the influence of dissipation on the controllability of the ET reaction the coupling strength, i.e., the magnitude of the bath spectral density $J(\omega)$ (see Appendix A) will be varied.

Before giving a detailed analysis of the control task, we

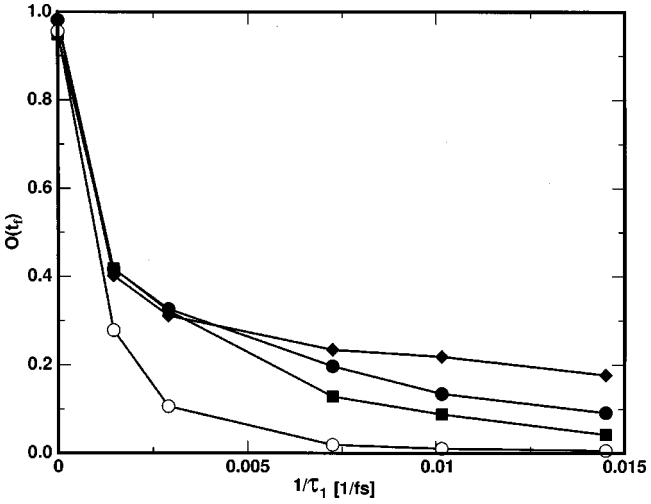

FIG. 3. ET control efficiency for model I-2 in dependence on the inverse lifetime of the target vibronic state (system parameters according to Table I). Curves for different values of the penalty factor λ, Eq. (13) are drawn. Filled squares: λ=1, filled circles: λ=1/5, and filled diamonds: λ=1/20. For comparison the efficiency is shown which is achieved in applying the optimal pulse valid for the absence of dissipation (open circles). (λ in units of $\mathrm{cm}^2\,\mathrm{V}^{-2}\,\mathrm{s}$).

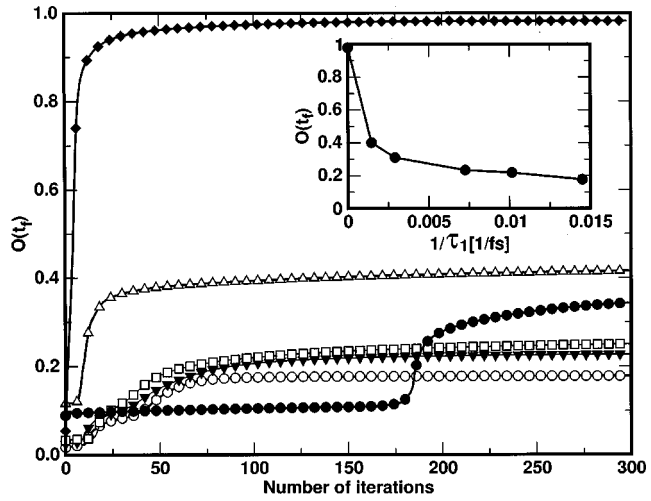

FIG. 4. ET control efficiency for model I-1 in dependence on the number of iteration steps taken to solve the OC equations (system parameters according to Table I). Curves for different inverse lifetimes of the vibronic target state are shown. Filled diamonds: $1/\tau_s=0$, empty triangles: $1/\tau_s=1.45\times10^{-3}$/fs, filled circles: $1/\tau_s=2.9\times10^{-3}$/fs, empty squares: $1/\tau_s=7.25\times10^{-3}$/fs, filled triangles: $1/\tau_s=1.01\times10^{-2}$/fs, and empty circles: $1/\tau_s=1.45\times10^{-2}$/fs. Insert: Final control yield as a function of the target state inverse vibrational lifetime.

try to characterize the general importance of laser-pulse control at the presence of dissipation. Usually the counterproductive influence of dissipation is emphasized while trying to control molecular dynamics. Figure 3 put this into a more quantitative frame. There we have drawn the control efficiency $O(t_f)$ versus the strength of dissipation represented by an increasing decay rate of the target state (decreasing vibrational lifetime τ_{A1} of the first excited vibrational state at the acceptor). To distinguish between different laser-pulse intensities, the penalty factor λ has been varied, too. All these curves have to be compared with a curve which is obtained without applying the OC theory at the presence of dissipation. What has been only done to get this reference curve is to take the pulse which solves the OC theory in the absence of dissipation and to calculate the control efficiency $O(t_f)$ while increasing dissipation. As can be seen from Fig. 3, the application of the OC theory at the presence of dissipation may drastically increase the control efficiency, in particular for an intermediate influence of vibrational relaxation and the largest applied laser-pulse intensities. If a generalization to other types of molecular systems might be possible, the promising result can be stated that laser-pulse control for condensed phase situations would really make sense although the given control task cannot be solved completely.

To get more insight into the convergency behavior of the OC algorithm, we proceed as in Fig. 2 and show in Fig. 4 the control yield $O(t_f)$ in its dependence on the number of iteration steps. And, indeed, the dissipationless case shows the same rapid convergency as it could be already observed in Fig. 2. In contrast, the presence of dissipation results in a somewhat slower convergency which behaves unpredictably and even nonmonotonously. And, more iteration steps become necessary. But in any case, more than 90% of the final yield is achieved within about 50 iteration steps (except the curve with a second threshold at about 170 steps). According to our observations, this seems to be a universal property of the used iteration procedure, again indicating that the solution of the OC problem may be locked in a local minimum.

Any computation mentioned so far leaves a corresponding optimal laser field. Those related to the calculations of Fig. 3 have been displayed in Fig. 5. In the absence of dissipation an almost 100% population of the target state is achieved. The laser field extends over the whole interval (t_0,t_f) having enough time to adjust the wave-packet motion over the exited PES in order to populate the desired target state at the given time. If dissipation starts to act, we observe a concentration of the control field to larger times and a change of some features. The latter behavior is caused by the reduced wave-packet motion when increasing the strength of dissipation.

The time evolution of the electronic and vibrational state populations related to the laser pulses given in Fig. 5 are shown in Fig. 6. If dissipation is absent, one observes a periodic motion of the population between the donor and ac-

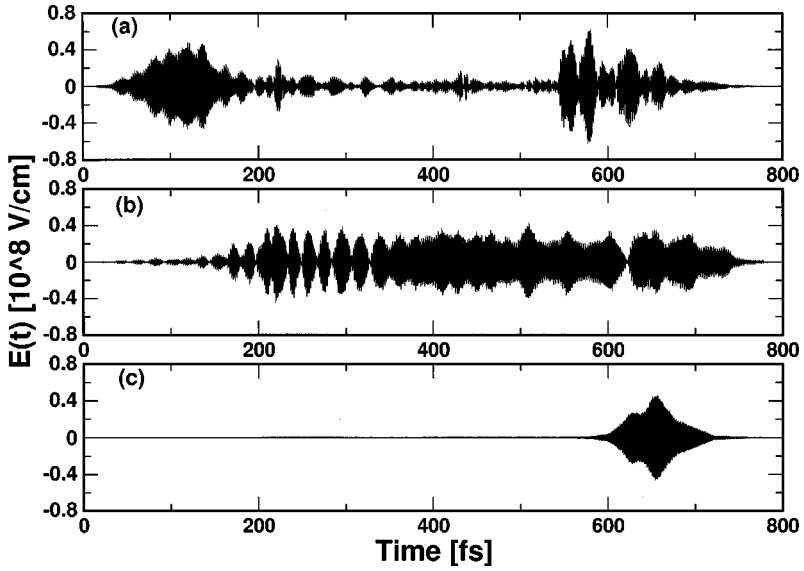

FIG. 5. Laser pulse control of ET for the model I-2 (system parameters according to Table I). The optimal pulse is shown for control tasks which differ with respect to the lifetime of the target state. Panel a: isolated system, panel b: small dissipation, and panel c: medium dissipation.

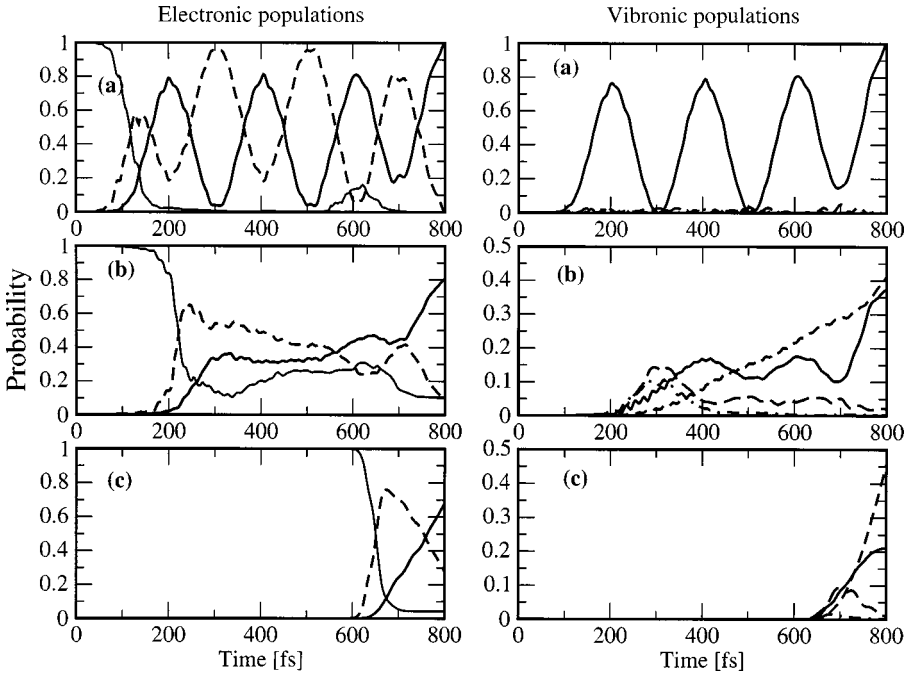

FIG. 6. Populations of the electronic states (left) and of the vibrational levels in the acceptor state (right) vs time for the ET model I and for the optimal pulses given in Fig. 5. Left part: electronic ground state (thin full line), excited donor state (dashed line), acceptor state (full line). Right part: acceptor vibrational ground state (dashed line), first excited vibrational state (target state, full line), second excited vibrational state (long dashed line), and third excited vibrational state (dash-dotted line).

ceptor level. After two periods of this motion an almost complete population is achieved of the excited state PES, exhibiting at some points nearly 100% population of the donor excited level, but only about 80% population of the desired acceptor state. From the corresponding part of Fig. 6 displaying vibrational populations we see that within the target electronic state, the whole population is already concentrated on the target vibronic level. Finally, we notice the action of the pulse near the end of the control interval which removes the part of the wave packet trapped in the donor level and achieves the complete population of the target state. This is a behavior characteristic for the completely coherent motion of the system. Specially shaped wave packets are iteratively improved while they move coherently on the excited PES.

In Figs. 6(b) and 6(c), the populations are shown for an increasing strength of dissipation. Due to the loss of coherence, the algorithm cannot rely on iterative improvement of the wave packet. Instead, the action of the laser pulse concentrates to later times to avoid the depopulation of the target level. In the case of medium dissipation [Fig. 6(b)] the excited donor level is populated first around $t=200$ fs. And in contrast to the dissipationless case where population has been directly transferred into the target vibronic level, now population is also transferred into two levels positioned above the target level (here the first excited vibrational level). According to the vibrational relaxation these higher-lying levels are later depopulated into the target state and in this way they contribute to its population.

We may also note that the population of the target level still preserves some oscillatory features from the dissipationless case. However, these traces of the coherent dynamics are lost if dissipation is further increased and the OC algorithm avoids earlier excitations completely. The whole population is transferred into the target state during the last 200 fs. Looking at the vibronic populations, it can be again concluded that a substantial portion of the target state population comes from the decay of higher-lying vibrational levels. So our general observation is, that the OC algorithm finds an alternative route to solve the control problem when the strength of dissipation increases. Due to this fact the optimal field computed for the absence of dissipation, although having higher pulse energy, fails to guide the dissipative dynamics (cf. Fig. 3).

It is of some interest to compare the result of the OC calculations with the dynamics free of any external control following an ultra-short laser pulse excitation (compare Fig. 7 with Fig. 6). We immediately notice significant differences in the dynamics of the dissipationless case already found in Ref. 26. Due to the lack of dissipation, ET proceeds coherently with comparatively low population of the acceptor level, where mainly higher excited vibronic levels are populated [Fig. 7(a), right]. The population of the target vibronic state is negligible. With increasing dissipation the dynamics in both cases becomes more similar for the electronic populations. The vibronic populations, however, show still signs of the coherent motion in the control case, in contrast to the case without a control field. The maximum population of the target level achieved around the middle of the studied time window (about 25%) is smaller than that achieved if the laser-pulse control has been carried out (more than 35%). For higher coupling strengths to the environment the results without a control field and in the presence of such a field become almost identical, except for the shift to later times in the case external-field control. A short laser pulse populating the target state in the shortest possible time is close to the optimum for this particular case.

C. Interplay of vibrational relaxation and internal conversion (ET Model II)

In this final section we will consider ET control using model II which represents a minimal model for the internal

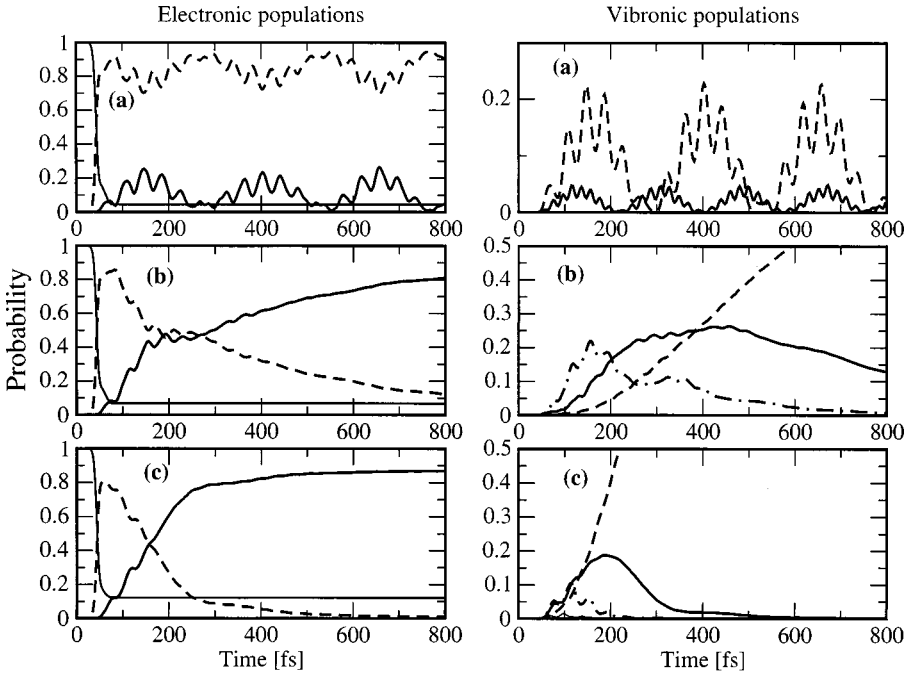

FIG. 7. Populations of the electronic states (left) and of the vibrational levels in the acceptor state (right) versus time for the ET model I and for an excitation with 50 fs long Gaussian laser pulse. Left part: electronic ground state (thin full line), excited donor state (dashed line), acceptor state (full line). Right part: (a) vibrational states with quantum numbers $N=2$ (full line) and $N=3$ (dashed line), (b) and (c) vibrational states as in Fig. 6.

conversion process observed in betaine-30. In the language of donor–acceptor ET the charge motion described in model II corresponds to ET in the inverted region. The final state of this ET would be the vibrational ground state in the S_0-state PES. However, to demonstrate the possible ET control we chose as a target state the third excited vibrational state in the S_1-state PES, i.e., $|\varphi_e\rangle|\chi_{e3}\rangle$. This state has been taken to have a target somewhat similar to that of the foregoing section, and it would allow to discuss laser-pulse stabilization of an excited state against internal conversion.

Again we start with a discussion of the convergence behavior of the OC algorithm what is displayed in Fig. 8. In comparison with ET model I, Fig. 4, the convergence seems to be rather fast, and already the initial guess for the laser pulse used to initialize the iterative OC algorithm (a simple Gaussian-shaped pulse) reaches a good result (see Fig. 9). On the other hand, the optimal field obtained when the iteration has been finished differs substantially from the initial guess and exhibits a rather complicated time dependence. This is due to the nonadiabatic coupling between the ground and the excited state. Apparently, the OC algorithm tries to compensate the fast oscillations caused by this coupling (see the initial part of the electronic populations given in Fig. 8). We can also observe, that these oscillations almost disappear at later times. Since these oscillations have a small amplitude, their compensation only results in a small improvement of the control efficiency compared to the efficiency achieved with the initial guess for the laser pulse. Noting the insert in Fig. 8 we can state that a similar reduction of the control efficiency is obtained as for ET model I. And the optimal pulse shows a very similar tendency with an increasing strength of dissipation to concentrates at later times and to populate the target state via a depopulation of levels positioned above the target level.

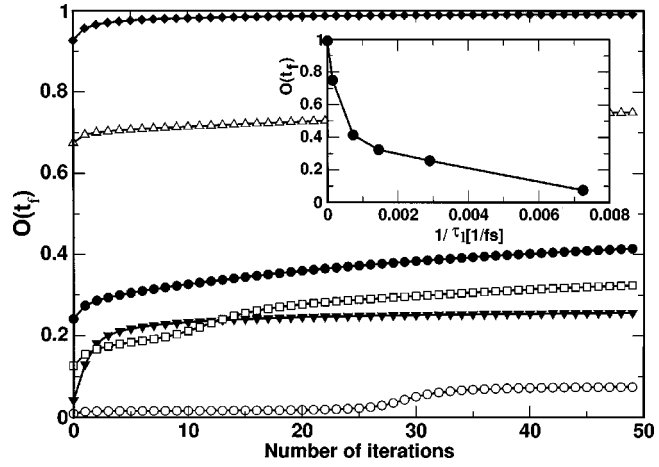

FIG. 8. ET control efficiency for model II in dependence on the number of iterations necessary to solve the OC equations (system parameters according to Table II). Curves for different inverse lifetimes of the target vibronic state are shown. Filled diamonds: $1/\tau_s=0$, empty triangles: 1.45^{-4}/fs, filled circles: 7.25×10^{-4}/fs, empty square: 1.45^{-3}/fs, filled triangles: 2.9×10^{-3}/fs, and empty circles: 7.25×10^{-3}/fs. Insert: control yield versus the inverse lifetime of the first excited vibrational level.

The laser-guided dynamics obtained from the OC theory has also been compared with the dynamics following after a short excitation with a Gaussian-shaped pulse with pulse width $\tau_p=20$ fs, and positioned at the corresponding Franck–Condon window. (This pulse has also been used as the guess field to start the OC algorithm.) The calculation demonstrates that the application of the OC theory leads to a significant enhancement of the yield compared to that obtained by the 20 fs excitation. And, the calculations also prove that the laser-guided dynamics exhibits a rather organized motion of the population among the electronic levels which is in contrast to the motion one gets after the short excitation.[26]

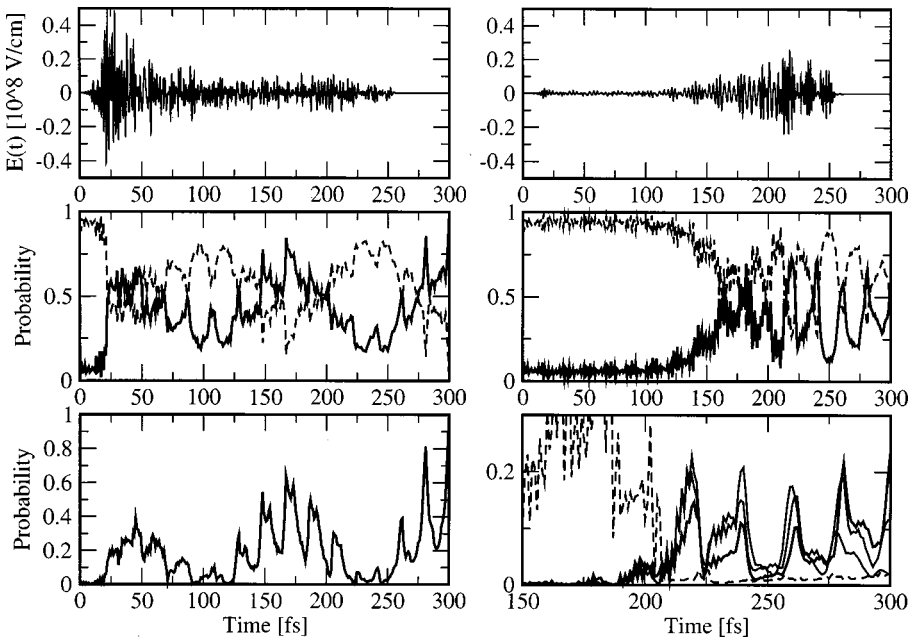

FIG. 9. ET control in the inverted region, model II. The figure shows the optimal pulse (top), the electronic level populations (center), and the vibronic level populations (bottom) for the case of the isolated system (left) and for the case with dissipation ($1/\tau_s = 2.9\times 10^{-3}$/fs) (right, note the changed scale for the vibrational level populations).

D. Acceleration of the OC algorithm convergency

As demonstrated in Fig. 4 the iteration algorithm for solving the OC theory may exhibit a fast convergence to a certain value of $O(t_f)$ where it remains for a comparatively high number of iteration steps. Later, a fast convergency follows to a somewhat larger value of $O(t_f)$. This behavior indicates that the OC algorithm has only found a local extremum. We shortly explain how to circumvent such a pinning in a local extremum, and in this manner, how to accelerate the iteration procedure.

The idea here is to randomly add some fluctuations to the control field during the iterative solution of the OC problem. Such a procedure should check whether or not a local optimum is occupied. The easiest way to introduce such fluctuations which perturb the OC algorithm is first to generate a Gaussian pulse of random duration, intensity, frequency and position in time, and second, to add this pulse to the obtained iterative version of the optimal pulse.

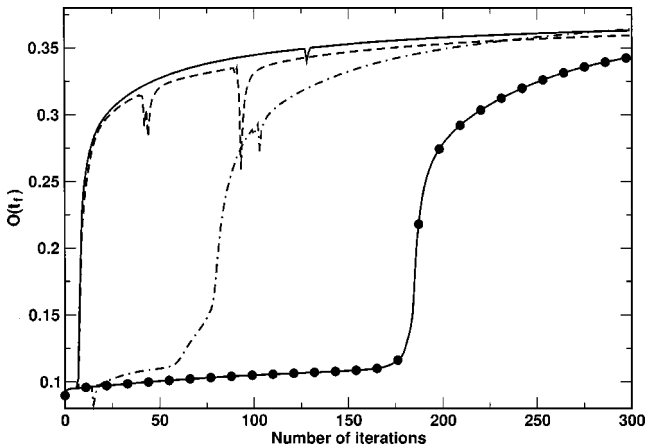

FIG. 10. Convergency behavior of the OC algorithm extended by random fluctuations. Model I-1 with $1/\tau_s = 2.9\times 10^3$/fs. Fluctuations are applied for 10 successive iterations beginning at the 3rd one (full line, dashed line) as well as the 15th one (dot-dashed line) to induce the transition to the higher optimum, and beginning from the 35th one, the 80th one (dashed line), the 100th one (dot-dashed) as well as the 125th (full line) to check the stability of the extremum. For comparison, the result is plotted which follows if any additional contribution to the approximate version of the optimal pulse is neglected (full line with filled circles).

The results of our computations for ET model I-1 are summarized in Fig. 10. The fluctuation of the approximate version of the optimal pulse has been introduced within 10 successive iteration steps starting from the third iteration (full and dashed lines in Fig. 10) and the 30th iteration (dot–dashed line in Fig. 4), respectively. As it is obvious the procedure moves the solution of the OC problem away from the local extremum, and in all cases the speed of convergency has been significantly enhanced as compared to the ordinary iterative computations. Furthermore, the value for $O(t_f)$ reached after about 150 iterations is even higher than that obtained after 300 iterations following the standard way. If further fluctuations are applied for later iterations a temporary decrease of the OC efficiency appears, but after a few iterations the result continues to converge to the original value. This shows the stability of the extremum, which then can be more likely the global one. But the behavior of the standard OC algorithm in this case indicates that it also converges to a global extremum. This indicates that the results presented in the foregoing sections remain valid, possibly with a somewhat large value of $O(t_f)$. We believe that the introduction of random fluctuation into the ordinary OC scheme can be used in general to enhance the convergency and to check the stability of the reached extremum. Respective work to design a general scheme is under way.

V. CONCLUSIONS

The present paper has been aimed to give a consistent theoretical formulation of the optimal control problem in the presence of excitation energy dissipation as well as dephasing and to apply this to different types of ultrafast ET reac-

tions. Based on the optimal control equations valid for the reduced density operator of the system and an auxiliary density operator describing back propagation in time, the behavior of the iterative algorithm used to solve the control task could be analyzed. It has been demonstrated that a laser-pulse controllability is possible of ET reactions (under the influence of a dissipative environment). The yield computed for all considered control tasks would be large enough for a successful experimental verification.

Although the control efficiency decreases with an increase of the system-environment coupling it has been shown that laser-pulse control may partially act against the counterproductive influence of dissipation. This indicates that laser-pulse control of ET reactions (and other types of ultrafast phenomena) is really a promising attempt even if carried out at condensed phase conditions. For such types of control tasks it would be really desirable to have a criterion at hand which offers an upper limit for the control yield one can achieve at a given strength of dissipation. Respective investigations are in progress.

ACKNOWLEDGMENTS

The authors gratefully acknowledge financial support by the Deutsche Forschungsgemeinschaft especially through Sonderforschungsbereich 450.

APPENDIX A: REDUCED DENSITY OPERATOR EQUATIONS

A formal solution of the density operator equation has been given in Eq. (10) by introducing the time-evolution superoperator $\mathcal{U}$. The concrete type of equation related to $\mathcal{U}$ should be taken here in the standard form of the so-called Markovian Quantum Master Equation (see e.g., Ref. 29)

$$\frac{\partial}{\partial t}\hat{\rho}(t) = -i\mathcal{L}_{\rm mol}\hat{\rho}(t) - i\mathcal{L}_{\rm F}(t)\hat{\rho}(t) - \mathcal{D}\hat{\rho}(t). \tag{A1}$$

The $\mathcal{L}_{\rm mol}$ and $\mathcal{L}_{\rm F}$ are the Liouville superoperators corresponding to the commutator with $H_{\rm mol}$, Eq. (1) and $H_{\rm F}$, Eq. (4), respectively. All effects following from the coupling to the environment are comprised in the action of the dissipative superoperator[29,47]

$$-\mathcal{D}\hat{\rho} = -\sum_a \left(\mathcal{K}_a\Lambda_a\hat{\rho} + \hat{\rho}\Lambda_a^+\mathcal{K}_a - \Lambda_a\hat{\rho}\mathcal{K}_a - \mathcal{K}_a\hat{\rho}\Lambda_a^+\right), \tag{A2}$$

with

$$\Lambda_a = \sum_b \int_0^\infty d\tau C_{ab}(\tau)U_{\rm mol}(\tau)\mathcal{K}_b U_{\rm mol}^+(\tau). \tag{A3}$$

We again remind on two approximations involved in the given form of the dissipative superoperator. First the influence of the external field has been neglected,[40] and the density operator equation has been reduced to the Markovian type (a discussion of non-Markovian effects in relation to fs-laser pulse excitation has been given in Ref. 48).

The reservoir correlation functions appearing in Eq. (A3) reads $C_{ab}(t) = 1/\hbar^2 \times {\rm tr}_{\rm R}\{\hat{R}_{\rm eq}U_R^+\Phi_a U_R\Phi_b\}$. It is given as a trace with respect to the reservoir state space and refers to the thermal equilibrium described by the reservoir equilibrium statistical operator $\hat{R}_{\rm eq}$. Providing the reservoir degrees of freedom as uncoupled harmonic oscillators the reservoir correlation function takes the form $C_{ab}(t) = \int d\omega \exp(-i\omega t) \times (1+n(\omega))(J_{ab}(\omega) - J_{ab}(-\omega))$, where $n(\omega)$ denotes the Bose–Einstein distribution and the quantities $J_{ab}(\omega) = \Sigma_\xi k_\xi(a)k_\xi(b)\delta(\omega-\omega_\xi)$ represent the spectral densities of the reservoir normal modes (see, e.g., Ref. 29).

To obtain the electron-vibrational state representation of the density operator necessary for establishing Eq. (12), we will proceed stepwise. First we introduce a representation with respect to the electronic states φ_a, where $\hat{\rho}_{ab}(t) = \langle\varphi_a|\hat{\rho}(t)|\varphi_b\rangle$ is just an operator in the vibrational state space. We do not give the complete equation-of-motion but restrict ourselves to the dissipative part

$$\begin{aligned}\langle\varphi_a|\mathcal{D}\hat{\rho}(t)|\varphi_b\rangle = \sum_c \big(&K_a\langle\varphi_a|\Lambda_a|\varphi_c\rangle\hat{\rho}_{cb}(t) \\ &+ \hat{\rho}_{ac}(t)\langle\varphi_c|\Lambda_b^+|\varphi_b\rangle K_b \\ &- \langle\varphi_a|\Lambda_b|\varphi_c\rangle\hat{\rho}_{cb}(t)K_b \\ &- K_a\hat{\rho}_{ac}(t)\langle\varphi_c|\Lambda_a^+|\varphi_b\rangle\big).\end{aligned} \tag{A4}$$

This expression has to be used to write down the electron-vibrational representation of the density operator equations as given in Eq. (12). Here, we only demonstrate how to get the respective dissipative contributions. In using Eq. (A4) the electron-vibrational representation reads

$$\begin{aligned}&\langle\chi_{aM}|\langle\varphi_a|\mathcal{D}\hat{\rho}(t)|\varphi_b\rangle|\chi_{bN}\rangle \\ &= \sum_c \sum_{\bar{M},\bar{N}} \big(K_{aM,a\bar{M}}\Lambda^{(a)}_{a\bar{M},c\bar{N}}\rho_{c\bar{N},bN}(t) \\ &\quad + K_{b\bar{N},bN}\Lambda^{(b)*}_{b\bar{N},c\bar{M}}\rho_{aM,c\bar{M}}(t) - K_{b\bar{N},bN}\Lambda^{(b)}_{aM,c\bar{M}}\rho_{c\bar{M},b\bar{N}}(t) \\ &\quad - K_{aM,a\bar{M}}\Lambda^{(a)*}_{bN,c\bar{N}}\rho_{a\bar{M},c\bar{N}}(t),\end{aligned} \tag{A5}$$

where the $K_{aM,aN}$ stand for the vibrational matrix elements $\langle\chi_{aM}|K_a|\chi_{aN}\rangle$, and we introduced $\Lambda^{(c)}_{aM,bN} = \langle\chi_{aM}|\langle\varphi_a|\Lambda_c|\varphi_b\rangle|\chi_{bN}\rangle$ as the electron-vibrational matrix element of the Λ-operators, Eq. (A3).

While the calculation of $\Lambda^{(c)}_{aM,bN}$ is possible in a direct way for ET model II, one has to change for ET model I to the adiabatic representation of the donor–acceptor states. Therefore we take the adiabatic state matrix elements of the time-dependent $\mathcal{K}$-operator as appearing in Eq. (A3)

$$\langle\psi_\alpha|U_{\rm mol}(\tau)\mathcal{K}_b U_{\rm mol}^+(\tau)|\psi_\beta\rangle = e^{-i\omega_{\alpha\beta}\tau}\langle\psi_\alpha|\mathcal{K}_b|\psi_\beta\rangle, \tag{A6}$$

where the $\omega_{\alpha\beta}$ denote transition frequencies among adiabatic levels. Inserting this into Eq. (A3) gives the correct expression for the diabatic state matrix elements of the Λ-operator

$$\begin{aligned}\Lambda^{(c)}_{aM,bN} &= \frac{1}{2}\sum_d \sum_{\alpha,\beta} C_{cd}(-\omega_{\alpha\beta})A_\alpha(aM)A_\beta^*(bN) \\ &\quad \times\langle\psi_\alpha|\mathcal{K}_d|\psi_\beta\rangle \\ &= \frac{1}{2}\sum_d \sum_{\alpha,\beta} (1+n(\omega_\alpha))(J_{cd}(\omega_{\beta\alpha}) \\ &\quad - J_{cd}(\omega_{\alpha\beta}))A_\alpha(aM)A_\beta^*(bN)\langle\psi_\alpha|\mathcal{K}_d|\psi_\beta\rangle.\end{aligned} \tag{A7}$$

The remaining matrix element can be expressed by diabatic state matrix elements

$$\langle \psi_\alpha | \mathcal{K}_d | \psi_\beta \rangle = \sum_{K,L} A^*_\alpha(dK) A_\beta(dL) K_{dK,dL}\,. \tag{A8}$$

Once the Hamiltonian Eq. (1) referring to the ET model I has been diagonalized, the adiabatic energies and expansion coefficients can be used to compute the complete dissipative part of the density matrix equations.

APPENDIX B: BACKWARD PROPAGATION

It has been discussed in detail in Ref. 26 how to obtain a density operator equation which realizes the backward propagation introduced in Eq. (18). As a result one obtains

$$\frac{\partial}{\partial t}\hat{\sigma}(t) = -i\mathcal{L}_{\mathrm{mol}}\hat{\sigma}(t) - i\mathcal{L}_{\mathrm{F}}(t)\hat{\sigma}(t) + \tilde{D}\hat{\sigma}(t), \tag{B1}$$

with the dissipative part

$$\tilde{D}\hat{\sigma}(t) = \sum_a \left(\Lambda_a^+ \mathcal{K}_a \hat{\sigma}(t) + \hat{\sigma}(t)\mathcal{K}_a\Lambda_a - \Lambda_a^+ \hat{\sigma}(t)\mathcal{K}_a - \mathcal{K}_a\hat{\sigma}(t)\Lambda_a\right), \tag{B2}$$

which is essentially different from $\mathcal{D}$, Eq. (A2). First, we give the expansion with respect to the electronic states

$$\begin{aligned}\langle \varphi_a | \mathcal{D}\hat{\sigma}(t) | \varphi_b \rangle = \sum_c \big(&\langle \varphi_a | \Lambda_c^+ | \varphi_c \rangle K_c \hat{\sigma}_{cb}(t) \\ &+ \hat{\sigma}_{ac}(t) K_c \langle \varphi_c | \Lambda_c | \varphi_b \rangle \\ &- \langle \varphi_a | \Lambda_b^+ | \varphi_c \rangle \hat{\sigma}_{cb}(t) K_b \\ &- K_a \hat{\sigma}_{ac}(t) \langle \varphi_c | \Lambda_a | \varphi_b \rangle \big).\end{aligned} \tag{B3}$$

If confronted with Eq. (A4), one notes differences between dissipation in the course of forward and backward propagation which not only results from hermitian conjugations. In analogy to the change from Eq. (A4) to Eq. (A5) we get from Eq. (B3) the complete diabatic electron-vibrational representation of the action of the dissipative superoperator for the backward propagation.

$$\begin{aligned}&\langle \chi_{aM} | \langle \varphi_a | \tilde{\mathcal{D}}\sigma(t) | \varphi_b \rangle | \chi_{bN} \rangle \\ &= \sum_c \sum_{\bar{M},\bar{N}} \big(K_{c\bar{M},c\bar{N}} \Lambda^{(c)*}_{c\bar{M},aM} \sigma_{c\bar{N},bN}(t) \\ &\quad + K_{c\bar{M},c\bar{N}} \Lambda^{(c)}_{c\bar{N},bN} \sigma_{aM,c\bar{M}}(t) \\ &\quad - K_{b\bar{N},bN} \Lambda^{(b)*}_{c\bar{M},aM} \sigma_{c\bar{M},b\bar{N}}(t) \\ &\quad - K_{aM,a\bar{M}} \Lambda^{(a)}_{c\bar{N},bN} \sigma_{a\bar{M},c\bar{N}}(t) \big).\end{aligned} \tag{B4}$$

The various matrix elements of the Λ-operators have to be calculated as explained in the foregoing section.

[1] S. A. Rice and M. Zhao, *Optical Control of Molecular Dynamics* (Wiley, New York, 2000).
[2] D. J. Tannor, R. Kosloff, and S. A. Rice, J. Chem. Phys. **85**, 5805 (1986).
[3] P. Brumer and M. Shapiro, Chem. Phys. Lett. **126**, 54 (1986).
[4] A. P. Pierce, M. A. Dahleh, and H. Rabitz, Phys. Rev. A **37**, 4950 (1988).
[5] S. Shi, A. Woody, and H. Rabitz, J. Chem. Phys. **88**, 6870 (1988).
[6] Y. J. Yan, R. E. Gillian, R. M. Whitnell, K. R. Wilson, and S. Mukamel, J. Phys. Chem. **97**, 2320 (1993).
[7] A. Bartana, R. Kosloff, and D. J. Tannor, J. Chem. Phys. **99**, 196 (1993).
[8] Y. Ohtsuki, W. Zhu, and H. Rabitz, J. Chem. Phys. **110**, 9825 (1999).
[9] W. Zhu, J. Botina, and H. Rabitz, J. Chem. Phys. **108**, 1953 (1998).
[10] W. Zhu and H. Rabitz, J. Chem. Phys. **109**, 385 (1998).
[11] T. Baumert and G. Gerber, Isr. J. Chem. **34**, 103 (1995).
[12] A. H. Zewail, Adv. Chem. Phys. **101**, 3 (1997).
[13] Kent Wilson, Festoschrift, J. Chem. Phys. A **103**, 10021 (1999).
[14] Special issue on laser pulse control, Chem. Phys. **2001**, 267.
[15] T. Brixner, N. H. Damrauer, P. Niklaus, and G. Gerber, Nature (London) **414**, 57 (2001).
[16] R. S. Judson and H. Rabitz, Phys. Rev. Lett. **68**, 1500 (1992).
[17] K. Sundermann, H. Rabitz, and R. de Vivie-Riedle, Phys. Rev. A **62**, 013409 (2000).
[18] T. Mančal and V. May, Chem. Phys. Lett. (submitted).
[19] Y. Dakhnovskii, J. Chem. Phys. **100**, 6492 (1994).
[20] Y. Dakhnovskii and R. D. Coalson, J. Chem. Phys. **103**, 2908 (1995).
[21] Y. Dakhnovskii, D. G. Evans, H. J. Kim, and R. D. Coalson, J. Chem. Phys. **103**, 5461 (1995).
[22] I. A. Goychuk, E. G. Petrov, and V. May, Chem. Phys. Lett. **253**, 428 (1996).
[23] I. A. Goychuk, E. G. Petrov, and V. May, J. Chem. Phys. **106**, 4522 (1997).
[24] M. Grifoni and P. Hänggi, Phys. Rep. **304**, 229 (1998).
[25] J. T. York and Y. Dakhnovskii, J. Phys. Chem. B **105**, 8278 (2001).
[26] T. Mančal and V. May, Eur. Phys. J. D **14**, 173 (2001).
[27] J. M. Jean, R. A. Friesner, and G. R. Fleming, J. Chem. Phys. **96**, 5827 (1992).
[28] V. May and M. Schreiber, Phys. Rev. A **45**, 2868 (1992).
[29] V. May and O. Kühn, *Charge and Energy Transfer Dynamics in Molecular Systems* (Wiley-VCH, Weinheim, 1999).
[30] J. Jortner and M. Bixon, Adv. Chem. Phys. **106**, 107 (1999).
[31] K. Blum, *Density Matrix Theory and Application* (Plenum, New York, 1981).
[32] R. Kubo, M. Toda, and N. Hashitsume, *Statistical Physics II: Nonequilibrium Statistical Mechanics* Springer Series in Solid State Sciences Vol. 31 (Springer, Berlin, 1995).
[33] V. G. Bar'yakhtar and E. G. Petrov, *Kinetic Phenomena in Solids* (Naukova Dunka, Kiev, 1989).
[34] E. Fick and G. Sauermann, *The Quantum Statistics of Dynamic Processes* (Springer, Berlin, 1990).
[35] B. Burfeindt, C. Zimmermann, S. Ramakrishna, T. Hannappel, B. Meissner, W. Storck, and F. Willig, Z. Phys. Chem. (Munich) **212**, 67 (1999).
[36] C. Zimmermann, F. Willig, S. Ramkarishna, B. Burfeindt, B. Pettinger, R. Eichberger, and W. Storck, J. Phys. Chem. B **105**, 9245 (2001).
[37] R. Ramakrishna, F. Willig, and V. May, Phys. Rev. B **62**, R16330 (2000).
[38] S. Ramakrishna, F. Willig, and V. May, J. Chem. Phys. **115**, 2743 (2001).
[39] M. Schreiber, I. Kondov, and U. Kleinekathöfer, J. Lumin. **94**, 471 (2001).
[40] D. H. Schirrmeister and V. May, Chem. Phys. Lett. **297**, 383 (1998).
[41] U. Kleinekathöfer, I. Kondov, and M. Schreiber, Chem. Phys. **268**, 121 (2001).
[42] D. Egorova, A. Kühl, and W. Domcke, Chem. Phys. **268**, 105 (2001).
[43] K. Sundermann and R. de Vivie-Riedle, J. Chem. Phys. **110**, 1896 (1999).
[44] T. Mančal and V. May, Chem. Phys. **268**, 201 (2001).
[45] T. Mančal and V. May, Eur. Phys. J. B **18**, 633 (2000).
[46] C. Fuchs and M. Schreiber, J. Chem. Phys. **105**, 1023 (1996).
[47] O. Linden and V. May, Eur. Phys. J. D **12**, 473 (2000).
[48] T. Mančal and V. May, J. Chem. Phys. **114**, 1510 (2001).